Available online at www.sciencedirect.com
ScienceDirect
Polymer 48 (2007) 3584–3592
polymer
www.elsevier.com/locate/polymer

Influence of the adjustable parameters of the DPD on the global and local dynamics of a polymer melt

Flavien Lahmar*, Bernard Rousseau

Laboratoire de Chimie Physique, UMR 8000 CNRS, Bâtiment 349, Université Paris-Sud 11, 91405 Orsay Cedex, France

Received 21 February 2007; received in revised form 11 April 2007; accepted 13 April 2007
Available online 20 April 2007

Abstract

We present DPD simulations of linear polyethylene melts with force fields derived from microscopic simulations using the concept of potential of mean force. We aim at simulating realistic short polymers from a qualitative and quantitative point of view. An interesting issue is then to know the influence of the adjustable parameters of the DPD: γ, the friction coefficient, and r_C, the cut-off radius, on the global and local dynamics of the polymer, *i.e.*, the diffusion coefficient, D_{CM}, the end-to-end decorrelation time, τ_R and the Rouse times. By varying these two parameters, we investigate structural and dynamical properties for different polymeric systems at a given chain length. Although scaling laws typical of the Rouse model have been reproduced using this DPD method, we observe deviation from the Rouse theory for the local dynamics of certain systems. The dynamical properties of the polymer melt are defined simultaneously by γ and r_C. Therefore we combine these two parameters, introducing a new parameter, the effective friction coefficient, γ^{eff}.

Keywords: Mesoscopic simulations; Dynamics; Rouse model

1. Introduction

Polymer dynamics involve a large length scale and a wide range of time scales that atomic simulations cannot commonly attain. In the last decade, several coarse-grained descriptions have been developed to overcome this difficulty. The coarse-graining approach consists in integrating out the fast fluctuating variables of a certain number of microscopic units grouped in mesoscopic entity, called bead. By reducing the number of particles taken into account and the computational time, these methods permit to simulate much longer time scales and to have access to diffusion coefficient, end-to-end vector decorrelation time, and viscoelastic properties. The coarse-graining level can be few atoms [1–3], monomers [4–7] or a whole chain [8–10]. The way to obtain effective interactions differs in each case, going from iterative optimization procedures as the Coarse-Graining OPTimization method by Reith et al. [11] to more straightforward methods [7]. Depending on the coarse-graining level, different methods can be used to sample the phase space of the system. We use here dissipative particle dynamics (DPD) [12].

The DPD technique is based on the simulation of soft spheres whose motion is governed by conservative, dissipative, and random forces. In this work, we use a conservative force built using a potential of mean force approach. The conservative force field is determined from microscopic simulations [13]. This force field is used to reproduce a realistic polymer melt as far as structural properties are concerned. The dissipative and random forces act as a thermostat. They introduce adjustable parameters that have an impact on the dynamical properties of the polymer melt: the DPD friction coefficient, γ, and the cut-off radius, r_C.

Español and Serrano [14] discussed theoretically the behaviour of the dynamical properties of a DPD fluid. Groot and Warren [15] drew a direct link between the DPD friction and the diffusion coefficient in such a fluid. These systems are simple fluids where no conservative force is taken into account.

* Corresponding author.
E-mail address: flavien.lahmar@lcp.u-psud.fr (F. Lahmar).

0032-3861/$ - see front matter © 2007 Elsevier Ltd. All rights reserved.
doi:10.1016/j.polymer.2007.04.018

The situation is different in the present work, and we try to understand the relationship between the adjustable parameters of the dynamics, the resulting friction in the melt and the dynamical properties. Soddemann et al. [16] showed that using DPD as a thermostat in a MD simulation does not change the viscosity of the liquid, provided the DPD friction coefficient is not too high, that is, remains small compared to the intrinsic friction of the particles. In mesoscopic simulations where the potentials are soft, the intrinsic friction is low and the situation is totally different. We expect that the combination of the random and dissipative forces will lead the dynamics.

In this study we keep the coarse-graining level and the polymer length constant. We focus on the adjustable parameters of the dynamics that will affect the dynamical properties of the polymer melt. We study their influence on the diffusion coefficient and the end-to-end vector decorrelation time of the polymer. Furthermore, in order to have access to the local dynamics of the polymer chains, we compute the Rouse modes for different systems. We check that the local dynamics are in agreement with Rouse predictions and studied the influence of γ and r_C on the Rouse times. For certain systems we see a clear deviation from the Rouse theory.

In a recent paper, Kindt and Briels [17] studied scaling properties on dynamical properties of polymer melts. We want to know whether this method is applicable to our system. This kind of method could enable us to simulate a system at a given friction coefficient and to scale the obtained properties in order to have realistic values. This could permit us to have shorter computational time. We then try to apply a scaling method to the global and local dynamical properties.

This paper is organized as follows: in the first part, we present the principles of the DPD method. In a second part, we expose the main characteristics of the Rouse model and the concept of scaling on friction coefficient. In a third part, we present our results for the global and local dynamical properties and for the scaling method. Finally we introduce an effective friction coefficient γ^{eff} to combine the influence of γ and r_C into a single parameter, and we study the influence of this new parameter on the local and global dynamics of the melt.

2. The DPD simulation method

The DPD technique was first introduced by Hoogerbrugge and Koelman [12]. DPD is essentially a molecular dynamics simulation where the beads interact through direct conservative, dissipative and random forces. The equations of motion for a given bead have the following form:

$$\frac{\mathrm{d}\vec{r}_i}{\mathrm{d}t} = \frac{\vec{p}_i}{m_i} \tag{1}$$

$$\frac{\mathrm{d}\vec{p}_i}{\mathrm{d}t} = \sum_{i \neq j} \vec{F}^{\mathrm{C}}_{ij} + \vec{F}^{\mathrm{D}}_{ij} + \vec{F}^{\mathrm{R}}_{ij} \tag{2}$$

where $\vec{F}^{\mathrm{C}}_{ij}$ is the conservative force exerted on the ith bead by the jth bead, $\vec{F}^{\mathrm{D}}_{ij}$ is a dissipative force and $\vec{F}^{\mathrm{R}}_{ij}$ is a random force. An expression of the dissipative and random forces is:

$$\vec{F}^{\mathrm{D}}_{ij} = -\gamma \omega_{\mathrm{D}}(r_{ij})\left(\vec{e}_{ij} \cdot \vec{v}_{ij}\right)\vec{e}_{ij} \tag{3}$$

$$\vec{F}^{\mathrm{R}}_{ij} = \sigma \omega_R(r_{ij})\mathrm{d}W_{ij}\vec{e}_{ij} \tag{4}$$

where $\vec{e}_{ij} = (\vec{r}_i - \vec{r}_j)/\|\vec{r}_i - \vec{r}_j\|$ and $\vec{v}_{ij} = \vec{v}_i - \vec{v}_j$ with $\vec{r}_i$ and $\vec{v}_i$ being the position and velocity vectors of the bead i. $\mathrm{d}W_{ij}$ is a Gaussian white-noise term with $\mathrm{d}W_{ij} = \mathrm{d}W_{ji}$ and with the following properties:

$$\langle \mathrm{d}W_{ij}(t) \rangle = 0, \tag{5}$$

$$\langle \mathrm{d}W_{ij}(t)\mathrm{d}W_{i'j'}(t') \rangle = \left(\delta_{ii'}\delta_{jj'} + \delta_{ij'}\delta_{ji'}\right)\delta(t - t') \tag{6}$$

Español and Warren [18] showed that the following fluctuation–dissipation relation must be satisfied:

$$[\omega_{\mathrm{R}}(r)]^2\sigma^2 = 2\omega_{\mathrm{D}}(r)\gamma k_{\mathrm{B}}T \tag{7}$$

In practice, the following set of equations is retained:

$$\begin{cases} \omega_{\mathrm{R}}(r)^2 = \omega_{\mathrm{D}}(r) = \omega(r) \\ \sigma^2 = 2\gamma k_{\mathrm{B}}T \end{cases} \tag{8}$$

The weight function $\omega(r)$ provides the range of interaction for dissipative and random forces. In this work, this simple choice is made:

$$\omega(r) = \begin{cases} (1 - r/r_{\mathrm{C}})^2 & \text{for } r < r_{\mathrm{C}} \\ 0 & \text{else} \end{cases} \tag{9}$$

We will investigate the influence of the friction coefficient, γ, on the dynamical properties of the polymer. When studying dynamical regimes in the dissipative particle dynamics model, some authors like Español and Serrano [14] used normalized weight function and dimensionless parameters. In our case, the weight function is not normalized, therefore we expect that r_C will have an influence on the dynamical properties of our system. We want here to make clear that, when changing the value of the cut-off radius, we do not change the value of the density, that is, our simulations are not performed at a constant reduced density. When increasing r_C we increase the number of beads in interaction with each bead, but we also modify the weight function of our simulation. The influence of γ seems more simple but we should not forget that the dissipative force depends not only on γ but also on r_C through the weight function. Both the parameters then have an influence on the dynamical properties. We shall check that these parameters have no influence on the structure of the polymer melt.

For the conservative force, our approach consists in deriving conservative forces from a microscopic description. Mesoscopic particles were built onto microscopic particles [13]. In order to obtain force fields from microscopic interactions we

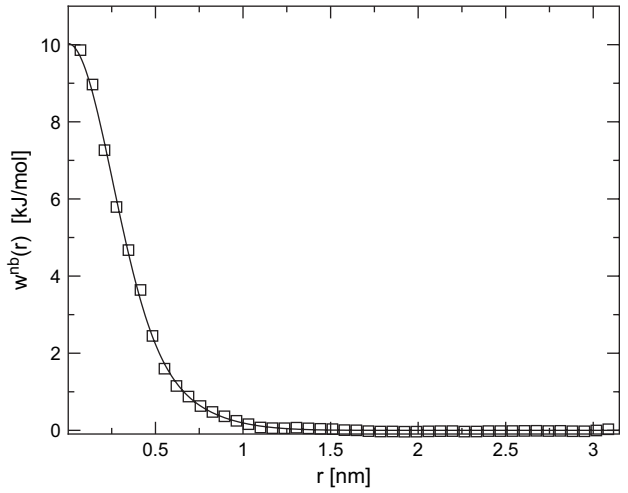

Fig. 1. Conservative non-bonded potential. The dotted line represents the fitting function.

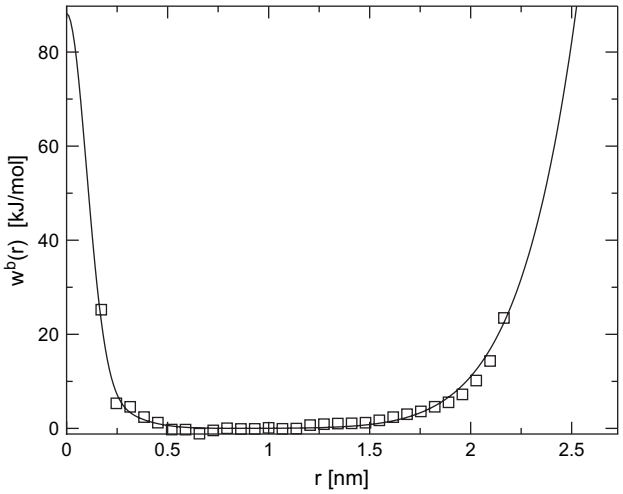

Fig. 2. Conservative bonded potential. The dotted line represents the fitting function.

use the concept of the potential of mean force. The expressions of the conservative forces are as follows:

$$\overrightarrow{F}_{ij}^{\mathrm{C,nb}} = -\nabla_i w^{\mathrm{nb}}(r_{ij}) \tag{10}$$

$$\overrightarrow{F}_{ii+1}^{\mathrm{C,b}} = -\nabla_i w^{\mathrm{b}}(r_{ii+1}) \tag{11}$$

with the potentials defined by:

$$w^{\mathrm{nb}}(r_{ij}) = -k_{\mathrm{B}}T \ln\left(g^{\mu,\mathrm{nb}}(r_{ij})\right) \tag{12}$$

$$w^{\mathrm{b}}(r_{ii+1}) = -k_{\mathrm{B}}T \ln\left(g^{\mu,\mathrm{b}}(r_{ii+1})\right) \tag{13}$$

$\overrightarrow{F}_{ij}^{\mathrm{C,nb}}$ is the non-bonded part of the conservative force and $\overrightarrow{F}_{ii+1}^{\mathrm{C,b}}$ is the bonded part. In these equations, μ refers to the results of Monte Carlo microscopic (*i.e.*, atomic) simulations. $g^{\mu,\mathrm{nb}}(r_{ij})$ and $g^{\mu,\mathrm{b}}(r_{ij})$ are pair distribution functions of the positions of coarse-grained particles mapped onto groups of microscopic particles.

The non-bonded potential is plotted in Fig. 1 and the bonded potential in Fig. 2. The potentials are fitted with Gaussian and power functions as follows:

$$w^{\mathrm{nb}}(r) = a_0 e^{-\left(\frac{r}{a_1}\right)^2} + a_2 e^{-\left(\frac{r}{a_3}\right)^2} \tag{14}$$

$$w^{\mathrm{b}}(r) = b_0 e^{-\left(\frac{r}{b_1}\right)^2} + b_2 e^{-\left(\frac{r}{b_3}\right)^2} + b_4 r^{b_5} \tag{15}$$

For more details concerning the mapping method and the parameters of the potentials, see Ref. [13].

3. Global and local Rouse dynamics

3.1. The Rouse Model

The Rouse model is considered as the standard model for the dynamics of unentangled polymer melts. It treats the motion of a Gaussian chain consisting of N beads with coordinates $\overrightarrow{R}_i(t)$ in a heat bath. For such a chain, equations of motion can be described by the following Langevin equations:

$$\zeta\frac{\mathrm{d}\overrightarrow{R}_1}{\mathrm{d}t} = -\frac{3k_{\mathrm{B}}T}{b^2}\left(\overrightarrow{R}_1 - \overrightarrow{R}_2\right) + \overrightarrow{F}_1^{\mathrm{R}} \tag{16}$$

$$\zeta\frac{\mathrm{d}\overrightarrow{R}_i}{\mathrm{d}t} = -\frac{3k_{\mathrm{B}}T}{b^2}\left(2\overrightarrow{R}_i - \overrightarrow{R}_{i-1} - \overrightarrow{R}_{i+1}\right) + \overrightarrow{F}_i^{\mathrm{R}} \tag{17}$$

$$\zeta\frac{\mathrm{d}\overrightarrow{R}_N}{\mathrm{d}t} = -\frac{3k_{\mathrm{B}}T}{b^2}\left(\overrightarrow{R}_N - \overrightarrow{R}_{N-1}\right) + \overrightarrow{F}_N^{\mathrm{R}} \tag{18}$$

where ζ is the segmental friction coefficient. The solution of the Rouse equations of motion is determined by transformation to its eigenmodes whose expressions are as follows:

$$\overrightarrow{X}_k(t) = \frac{1}{N}\sum_{i=1}^{N}\overrightarrow{R}_i(t)\cos\left(\frac{k\pi}{N}\left(i+\frac{1}{2}\right)\right) \quad k = 1,\ldots,N-1 \tag{19}$$

$\overrightarrow{X}_k$ represents the local motion of the chain which includes N/k segments. The self-correlation functions of these modes are given as:

$$\langle\overrightarrow{X}_k(t)\cdot\overrightarrow{X}_k(0)\rangle = \langle\overrightarrow{X}_k(0)^2\rangle\exp\left(-\frac{t}{\tau_k}\right) \tag{20}$$

with $\tau_k = \zeta b^2/[12k_{\mathrm{B}}T\sin^2(k\pi/2N)]$. The Rouse model also predicts:

$$\langle\overrightarrow{R}_{\mathrm{ee}}(t)\cdot\overrightarrow{R}_{\mathrm{ee}}(0)\rangle = 16\sum_{\mathrm{odds}}^{k\le N-1}\frac{b^2}{8N}\cot^2\left(\frac{k\pi}{2N}\right)\exp\left(-\frac{t}{\tau_k}\right) \tag{21}$$

For times longer than τ_{R}:

$$\langle \overrightarrow{R}_{ee}(t) \cdot \overrightarrow{R}_{ee}(0) \rangle \propto \exp\left(-\frac{t}{\tau_R}\right) \quad (22)$$

with $\tau_R = \zeta b^2 N^2 / 3\pi^2 k_B T$.

By integrating the equations of motion for the centre of mass, we can find that: $D_{CM} = k_B T / N\zeta$.

The scaling laws typical of the Rouse model are the following:

$$R_{ee} \propto N^{1/2} \quad (23)$$

$$D_{CM} \propto 1/N \quad (24)$$

$$T_R \propto N^2 \quad (25)$$

In this work, we do not consider entangled chains, so we will use the Rouse model as a reference and compare our results to those predicted by this model. We will compute the Rouse modes applying to the positions of the beads, and check whether these Rouse modes are the normal modes for our systems. Our aim is to check whether or not the DPD model behaves like the Rouse model at all relevant length scales.

3.2. Scaling on friction coefficient

In this paper we investigate the influence of the friction coefficient on the dynamical properties. In their mesoscale simulations, Kindt and Briels [17] used the concept of scaling on friction coefficient. We use here the same approach. If scaling applies to the DPD friction coefficient, all time-dependent properties must be similar *modulo* a scaling of the time axes. Considering a time-dependent property of a system simulated at a reference friction coefficient γ_0, we should obtain:

$$F_{\gamma_0}(t) = F_\gamma(ft) \quad (26)$$

with f depending linearly on γ.

Applying this scaling to the linear part of the mean-square displacements of the chains and to the autocorrelation function of the end-to-end vector we find that:

$$f(\gamma) = \frac{D_{CM}(\gamma_0)}{D_{CM}(\gamma)} \quad (27)$$

$$f(\gamma) = \frac{\tau_R(\gamma)}{\tau_R(\gamma_0)} \quad (28)$$

We can also apply this kind of scaling to the Rouse modes relaxation. We define a function $\alpha(\gamma)$ so that:

$$\tau_k = \frac{\alpha(\gamma)}{\sin^2\left(\frac{k\pi}{2N}\right)} \quad (29)$$

We then obtain another relation defining the scaling function:

$$f(\gamma) = \frac{\tau_k(\gamma)}{\tau_k(\gamma_0)} \quad k = 1, \ldots, N-1 \quad (30)$$

The Rouse theory predicts that $D_{CM} \propto 1/\zeta$ and $\tau_R \propto \zeta$. So this type of scaling applies directly to the Rouse friction coefficient, and we should find: $f(\zeta) = \zeta/\zeta_0$. Although the Rouse friction coefficient ζ and the DPD friction coefficient γ are different parameters, we try to find a similar scaling for the DPD friction coefficient and to find a relationship between these two coefficients. This relationship may depend on the cut-off radius of the considered system, r_C. This scaling could be very useful for our simulations. In order to simulate realistic polymers we should set γ at quite high value. This implies that the integration time step in the Velocity Verlet algorithm should be set at value lower than 10^{-5} ns. The concept of scaling could enable us to use lower friction coefficient, larger integration time step, and to observe all time-dependent properties on much shorter times.

4. Results

4.1. Systems and Simulation details

In this work we investigate polyethylene melts at a temperature of 450 K and a density of 0.761 g/cm^3. The number of chains, N_c, and the number of beads per chain, N_b, are kept constant ($N_c = 100$, $N_b = 10$). The level of coarse graining is $\lambda = 10$, *i.e.*, each bead represents $C_{20}H_{40}$. Because of this high coarse-graining level, the beads interact in a very soft manner and can interpenetrate. Thus, our simulations will only reproduce the Rouse regime and not show any presence of entanglements [19]. The DPD simulations were performed in the canonical ensemble (NVT) with minimum image convention. The integrator chosen was a modified Velocity Verlet as presented by Groot and Warren [15]. We have simulated systems with different cut-off radii, and, for each cut-off radius, different friction coefficients. The smallest value of r_C was defined such that $w^{nb}(r_C)/w^{nb}(0) = 5.5 \times 10^{-3}$. We used three values for r_C: 1.75, 2.25 and 2.75 nm. In comparison, the position of the first radial distribution function maximum is about 1 nm. Increasing r_C we increase the number of beads that are in interaction and consequently the computational time. We used seven different values of γ: 90, 135, 180, 225, 270, 315, 360 kg mol^{-1} ns^{-1}. Previous works on the same systems at different chain lengths showed that scaling laws typical of the Rouse model are reproduced using this approach [13].

4.2. Influence of the cut-off radius and friction coefficient on the global dynamics

For the different systems, we checked that the average of the kinetic energy of the system was equal to the expected one $\langle E_c \rangle = (3N/2)k_B T$ within a maximum error of 0.5%. For the range studied, the cut-off radius and the friction coefficient have no effect on the kinetic energy of the system, which is logical since the dissipative and random forces are linked by the relation of fluctuation–dissipation and act as a thermostat.

The structure of the chains is described by the radial distribution function, the chain end-to-end vector and the radius of

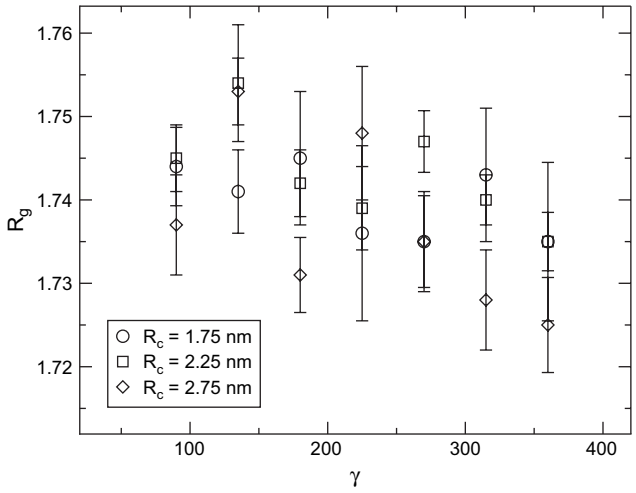

Fig. 3. Radius of gyration [nm] as a function of γ for the three cut-off values.

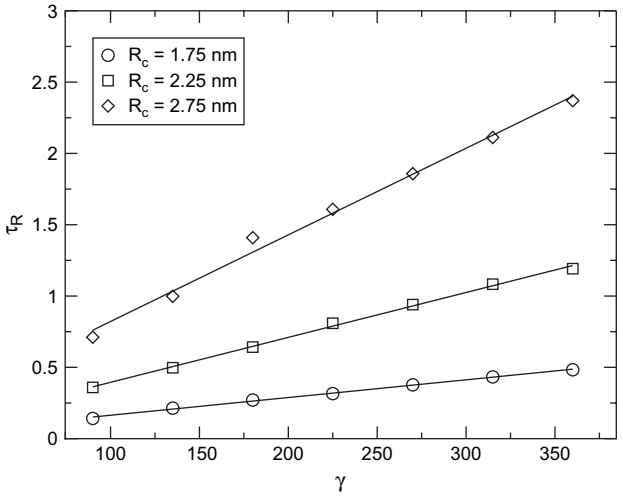

Fig. 5. τ_R [ns] as a function of γ for the three cut-off values.

gyration. The structure of the polymer is determined by the conservative forces and shall not depend on the friction coefficient. By changing the cut-off radius we change the range of the conservative forces and so this parameter could affect the structure of the polymer. Nevertheless, even for the smallest cut-off radius, the ratio $w^{nb}(r_C)/w^{nb}(0)$ is very small. We checked that the structural properties, the radial distribution functions, and the radius of gyration (plotted in Fig. 3) are not affected by the change of r_C and γ.

We now focus on the global dynamical properties of the polymer melt: the diffusion coefficient of the centre of mass, D_{CM}, and the decorrelation time of the end-to-end vector, τ_R.

D_{CM} is obtained from the slope of the long time behaviour of the mean-square displacement of the centre of mass:

$$D_{CM} = \lim_{t\to\infty} \frac{1}{6t}\langle[\vec{R}_{CM}(t) - \vec{R}_{CM}(0)]^2\rangle \tag{31}$$

Fig. 4 shows the evolution of D_{CM} with the friction coefficient for the three values of cut-off radius. As expected, the higher the friction coefficient is, the lower D_{CM} is. For $r_C = 2.25$ nm and $r_C = 2.75$ nm, we find that $D_{CM}(\gamma,r_C) \propto 1/\gamma$. For $r_C = 1.75$ nm, D_{CM} shows a different evolution: $D_{CM}(\gamma,r_C) \propto 1/\gamma^{0.8}$. In Fig. 4 we also see the influence of r_C on D_{CM}. The larger the r_C is, the lower the D_{CM} is. Although we have not investigated a large range of r_C we see that $D_{CM}(\gamma,r_C) \propto 1/r_C^{3,2}$. This influence is easy to understand: the greater the r_C is the more numerous are the beads in interactions with each bead and the greater is the dissipative force on each bead. But, we should not forget that the weight function is also involved in the computation of the dissipative force. The influence of r_C is then not only volumic. We will study this issue in the next section.

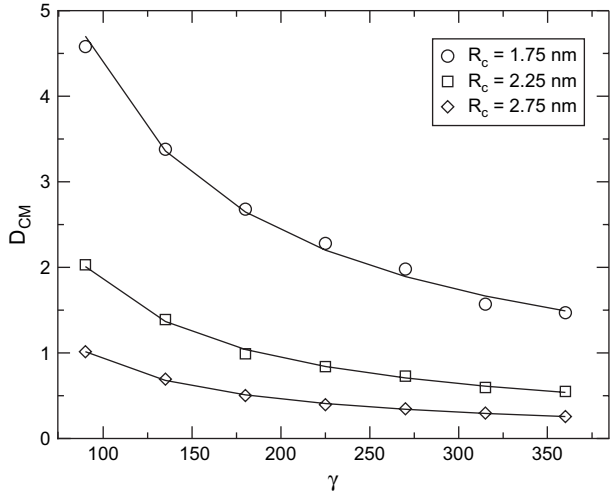

Fig. 4. D_{CM} [nm^2 ns^{-1}] as a function of γ for the three cut-off values.

To obtain τ_R, we fit the autocorrelation function of the end-to-end vector with the Rouse expression of the decorrelation end-to-end vector given in Eq. (22). Fig. 5 shows the evolution of τ_R with the friction coefficient for the three values of cut-off radius. As expected, the higher the friction coefficient is the higher the τ_R is. For the three values of r_C, we find that $\tau_R(\gamma,r_C) \propto \gamma$. We find the same kind of behaviour according to r_C as what was observed for the diffusion coefficient: $\tau_R(\gamma,r_C) \propto r_C^{3,2}$. For the two largest r_C values, our observations show that the dependence of the dynamical properties on γ is consistent with Rouse scaling laws on the friction coefficient. But it seems that the dependence on r_C is more complicated. We will now study the local dynamics of the polymer chains.

4.3. Local dynamics

The Rouse modes of the chains were studied for all systems. For realistic polymer chains, it is not expected that the Rouse modes are the normal modes. Indeed the uncrossability constraints and the non-bonded interactions modify the equations of motion and the dynamics of the polymer melt cannot be completely represented by the equations of the first section. In our work, we do not use uncrossability constraints but there are non-bonded interactions. We then expect that the Rouse modes may not relax exponentially. As in previous works

[20,21], we find that the Rouse mode autocorrelations can better be described by a stretched exponential form:

$$C_k(t) = \exp\left[-\left(t/\tau_k^*\right)^{\beta_k}\right] \tag{32}$$

where the relaxation times τ_k^* and the stretching parameters β_k depend on mode number k and on the DPD parameters. Having obtained the stretching parameters which characterize a deviation from the Rouse theory, we compute effective relaxation times using the Euler function:

$$\tau_k = \frac{\tau_k^*}{\beta_k}\,\Gamma\left(\frac{1}{\beta_k}\right) \tag{33}$$

In Fig. 6 we show the stretching parameters β_k as a function of the wavelength N/k for certain systems. Surprisingly certain systems show β_k greater than 1. For these systems we do not have stretched but compressed exponentials. This is not consistent with what is observed in lattice simulations of polymer chains without any uncrossability constraints [20]. For $r_C = 1.75$, we notice that the more we increase γ the closer β_k come to the value 1. In fact we observed two types of evolution of β_k according to N/k.

The first type of evolution is visible in Fig. 6. β_k is clearly above 1.0 for the smallest wavelengths. Then β_k decreases with N/k. This is not consistent with the Rouse theory. This shows that the choice of r_C and γ has an influence not only on the values of the dynamical properties but also on the dynamical mechanisms themselves. For other systems, the evolution is more consistent with what is observed in lattice simulations [20], in a qualitative way. We see a slight deviation from what is expected from the Rouse model, most of the stretching parameters are contained between 0.9 and 1.0. This slight, but physical, deviation can be due to the non-bonded interactions between the beads that are not taken into account in the Rouse model. To our opinion, the unphysical stretching parameters that we observe for certain systems are due to a too low resulting friction. This is not due only to r_C since we observe stretching parameters above 1.0 for ($r_C = 2.25$ nm, $\gamma = 90$) (see Fig. 6).

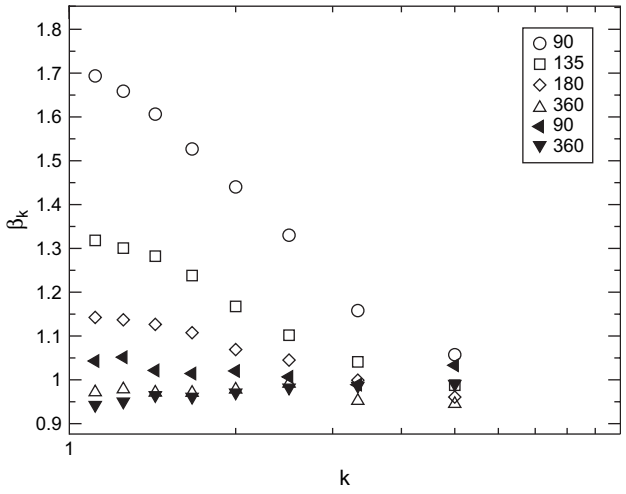

Fig. 6. Stretching parameters for the Rouse mode autocorrelations as a function of the wavelength N/k. Empty symbols represent results for $r_C = 1.75$ nm and filled symbols represent results for $r_C = 2.25$ nm.

For the different systems, we check Rouse predictions on τ_k. We find that the dependence on k has the following form:

$$\tau_k(\gamma) = \frac{\alpha(\gamma)}{\sin^x\left(\frac{k\pi}{2N}\right)} \tag{34}$$

with x varying between 1.9 and 2.0. In fact the α function encompasses a dependence on r_C, we should write $\alpha_{r_C}(\gamma)$. This expression is similar to what is expected from the theoretical Rouse model. In Fig. 7 we plot $\alpha(\gamma)$ for the three cut-off radius. These functions are linear, which is consistent with the theoretical expression of the Rouse times.

The study of the different systems suggests that there is a linear relation between the DPD friction coefficient γ and ζ, the corresponding Rouse friction coefficient. But it remains a dependence on r_C in these relations. The observation of the local dynamics shows that certain systems do not exhibit behaviour consistent with the Rouse model and that the choice of r_C and γ, in this regards, is of great importance in the DPD technique. We will now see whether a scaling method is applicable to our systems.

4.4. Scaling

Taking $\gamma_0 = 225$, we compute scaling functions as explained in the second section. If the scaling applies to all systems, all these functions, computed from the mean-square displacement, the relaxation time or the Rouse times should match. There should remain no dependence on r_C.

Fig. 8 displays this scaling for D_{CM}, τ_R and $\alpha(\gamma)$.

We can run a linear regression on the scaled coefficients of diffusion and relaxation times. In Fig. 8 we plot the regression lines computed from D_{CM}, τ_R and $\alpha(\gamma)$ functions. The regression lines are relatively close to each other, except the regression line for the diffusion coefficient of the first system

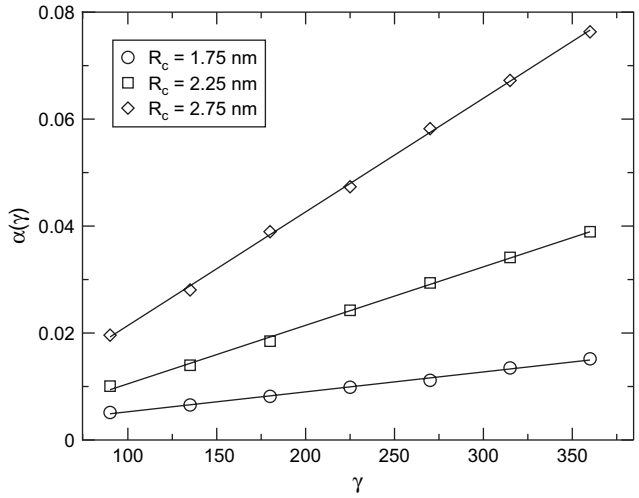

Fig. 7. α as a function of γ for the three cut-off radius.

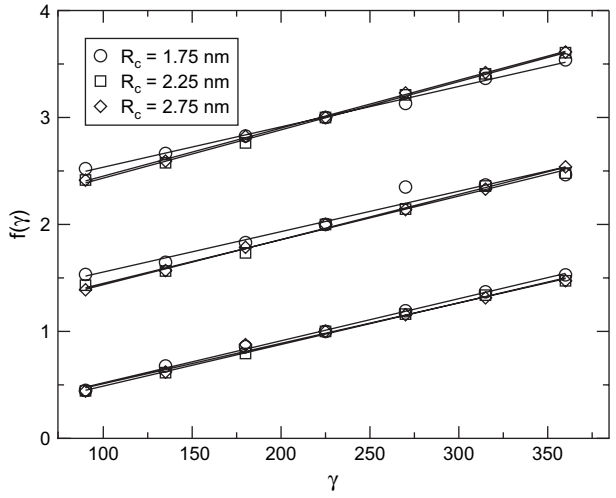

Fig. 8. Scaling function $f(\gamma)$ as a function of γ for the three cut-off values. For clarity reason, $f(\gamma)$ computed from the $\alpha(\gamma)$ function (above) and from the diffusion coefficient (in the middle) have been shifted.

($r_C = 1.75$ nm). For the $\alpha(\gamma)$ function, the line corresponding to the smallest r_C value differs from the others. Moreover, for this system, the slope of the regression lines for the diffusion coefficient, the Rouse times and the terminal time are different. This is not surprising given the clear deviation from the Rouse theory that we have observed for the local dynamics. For the two other systems, the results are much better. The regression lines do not show large differences and their slopes are close to $1/\gamma_0$. This method of scaling is then applicable to our technique for r_C larger than 1.75 nm.

5. Definition of a mean friction coefficient

We are confronted with a difficulty when trying to analyze our results as a whole. All the relations we can determine between γ, ζ, D_{CM} and τ_R are in fact dependent on r_C. We want to find a way of combining the dependence of r_C and the dependence of γ by using only one parameter. We have seen that the influence of r_C on the dynamical properties of our systems is partially due to a volumic phenomenon. Let us consider a bead in the polymer melt. By varying the cut-off radius, we change the mean number of beads that are in interaction with the first bead. But meanwhile, we change the weight function. In order to be able to quantify this effect we introduce a kind of mean friction coefficient, the *effective friction coefficient* defined as follows:

$$\gamma^{\text{eff}} = \int_0^{\infty} \gamma\omega(r, r_C) g(r, r_C) 4\pi r^2 \mathrm{d}r \tag{35}$$

In this definition, $g(r,r_C)$ is the radial distribution function and $\omega(r,r_C)$ is the weight function defined in the first section. We have seen that the radial distribution function that we obtain, when using quite large r_C, remains identical for all cut-off radius. We deduce a simpler form of γ^{eff}:

Table 1
Mean friction coefficient

r_C	γ^{eff}
1.75	$2.02 \times \gamma$
2.25	$4.52 \times \gamma$
2.75	$8.45 \times \gamma$

$$\gamma^{\text{eff}} = \gamma \int_0^{r_C} \left(1 - \frac{r}{r_C}\right)^2 g(r) 4\pi r^2 \mathrm{d}r \tag{36}$$

The second member of this equation is computed numerically thanks to the radial distribution function obtained from our simulations at each r_C.

It should be noticed here that, when no conservative forces are used, $g(r)$ is constant and equal to 1.0. The use of an effective friction coefficient as defined in Eq. (36) is then equivalent to the normalization of the weight function as proposed by Español and Serrano [14].

Table 1 summarizes the simple expression of γ^{eff} for the three cut-off radius.

This new parameter is very useful in our case because it enables us to plot the whole of our data on single curve unlike in the previous section. If we compute γ^{eff} for several r_C values we find that $\gamma^{\text{eff}} \propto r_C^{3.2}$, which is consistent with what we have observed in the previous section. It is evident from the definition of γ^{eff} that the relationship between couples (γ, r_C) and γ^{eff} is not injective. Several values of (γ, r_C) can give the same γ^{eff}. An interesting issue is then to know whether couples (γ, r_C) giving the same γ^{eff} give the same dynamical properties.

We now plot D_{CM} (Fig. 9), τ_R (Fig. 10) and α (Fig. 11) as functions of γ^{eff}. The first observation is that the data related to the three cut-off radius are located close to master curves that we have plotted on the corresponding figures. Nevertheless, the data corresponding to the lowest cut-off radius exhibit a somewhat different behaviour: the decrease of the diffusion

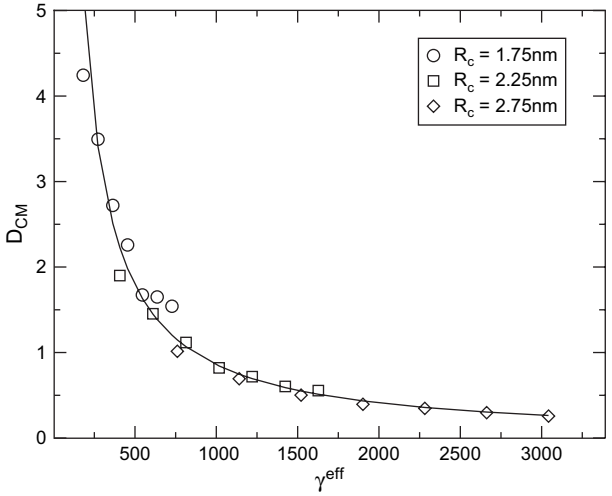

Fig. 9. Diffusion coefficient [$\text{nm}^2\,\text{ns}^{-1}$] of the centre of mass as a function of γ^{eff}.

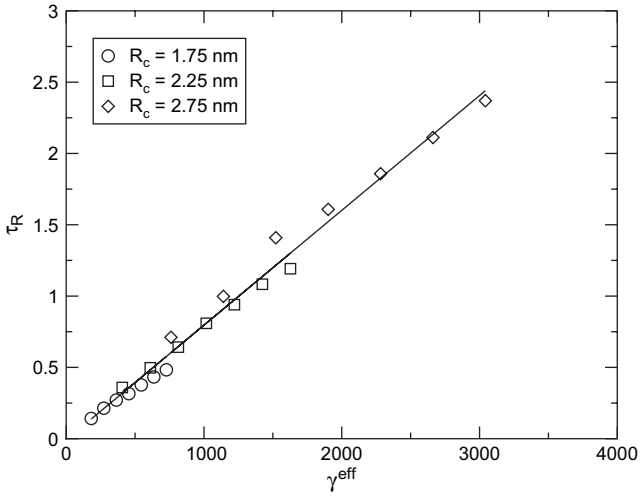

Fig. 10. End-to-end decorrelation times [ns] as a function of γ^{eff}.

coefficient is less rapid, the slopes are lower for the end-to-end decorrelation time and for the α function. We can also notice that the systems that show a deviation from the Rouse theory of local dynamics are those with the lowest effective friction coefficient. We should specify here that Langevin equations are applicable to the motion of a Rouse chain only for times greater than τ_i, defined as M/ζ. The Rouse theory shows that $\tau_i = MD_{\text{CM}}N/RT$. If we compute these times, we find that for $r_{\text{C}} = 1.75$ nm and $\gamma = 45$, $\tau_i = 3$ ps, which is of the order of the shortest Rouse times. Thus, for the systems with the lowest γ^{eff}, equations of motion of the shortest Rouse modes cannot be described by Langevin equations, and the deviation from the Rouse theory for certain systems is not really surprising. Nevertheless, we have no explanation for the unphysical local relaxations we observe. This only shows that one has to be very careful when choosing the parameters of the DPD if one wants to reproduce a correct local behaviour. We chose to run regressions on the data corresponding to $r_{\text{C}} = 2.25$ nm and $r_{\text{C}} = 2.75$ nm. We find that $D_{\text{CM}} \propto 1/(\gamma^{\text{eff}})^{1.09}$ and $\tau_{\text{R}} \propto (\gamma^{\text{eff}})^{1.05}$. If we look carefully at the different curves, we can notice that there still exists a small jump between the data for $r_{\text{C}} = 2.25$ nm and those for $r_{\text{C}} = 2.75$ nm. So there may remain a small dependence on r_{C} that is not linked to the volumetric effect that we have encompassed in γ^{eff}. The effective friction coefficient, however, enables us to understand the major part of the influence of r_{C} on the dynamical properties of the melt. It also enables us to simplify the link between the Rouse friction coefficient and the DPD friction coefficient. We know that the diffusion coefficient given by the Rouse model is as follows: $D_{\text{CM}} = k_{\text{B}}T/N\zeta$. We find from our data that $D_{\text{CM}} \propto 1/\gamma^{\text{eff}}$. This shows that there is a linear relation between ζ and γ^{eff}.

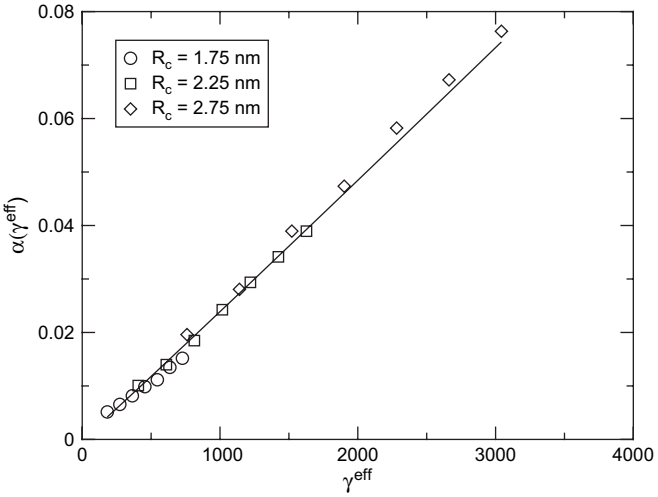

Fig. 11. α as a function of γ^{eff}.

6. Conclusion

We have investigated the dynamical properties of PE melts with DPD, varying simultaneously both adjustable parameters of the dynamics. Structural properties are not affected by the change of r_{C} and γ, provided we use large enough values of r_{C} and γ. The influence of these parameters is quite similar in a qualitative way. Increasing r_{C} increases the mean value of the dissipative force applied to the beads, which is comparable to what happened by an increase of γ. If we choose adjustable parameters corresponding to a low Rouse friction coefficient, we observe a clear deviation from the Rouse theory for local dynamics. This kind of strange behaviour would have an impact on the determination of viscoelastic properties of the melt. For systems that are in agreement with Rouse theory, from a local and global point of view, we have seen that there exists a linear relation between the DPD friction coefficient and the corresponding Rouse friction coefficient. But we shall not forget that these relations contain a dependence on r_{C}. For these systems, it is possible to apply a scaling method on the friction coefficient. The influence of r_{C} must be linked to the mean number of beads in interaction with each bead and to the weight function $\omega(r,r_{\text{C}})$. Therefore we introduce a new parameter, the effective friction coefficient that enables us to encompass the dependence on r_{C} and on γ into a single variable. This parameter permits to understand the major part of the influence of r_{C} on the dynamical properties and to build curves that can help us to determine the friction coefficient and the cut-off radius we should use in order to simulate polymers with given dynamical properties. The next step of this study could be the determination of the scaling of γ and r_{C} according to the coarse-graining level: when simulating a polymer melt at different coarse-graining levels, λ: how to choose γ and r_{C} in order to obtain the same dynamical properties at all λ? We expect that for coarse-graining level higher than $\lambda = 10$, we will keep a linear relation between the DPD friction coefficient and the corresponding Rouse friction coefficient. For an intermediate coarse-graining level, we expect that the intrinsic friction will play a major role in the dynamics and that the relationship between the DPD friction coefficient and the resulting friction in the polymer melt will not be linear anymore.

Acknowledgements

We are grateful to Michelin for financial support through a PhD grant for one of us (F.L.).

References

[1] Fukunaga H, Aoyagi T, Takimoto J-I, Doi M. Derivation of a coarse-grained potential for polyethylene. Comput Phys Chem 2001;142:224–6.
[2] Fukunaga H, Takimoto J, Doi M. A coarse-graining procedure for flexible polymer chains with bonded and nonbonded interactions. J Chem Phys 2002;116(18):8133–90.
[3] Tschöp W, Kremer K, Batoulis J, Bürger T, Hahn O. Simulation of polymer melts. I. Coarse-graining procedure for polycarbonates. Acta Polym 1998;49:61–74.
[4] Reith D, Meyer H, Müller-Plathe F. Mapping atomistic to coarse-grained polymer models using automatic simplex optimization to fit structural properties. Macromolecules 2001;34(7):2335–45.
[5] Faller R, Reith D. Properties of poly(isoprene): model building in the melt and in solution. Macromolecules 2003;36:5406–14.
[6] Akkermans RLC, Briels WJ. Coarse-grained dynamics of one chain in a polymer melt. J Chem Phys 2000;113(15):6409–22.
[7] Padding JT, Briels WJ. Uncrossability constraints in mesoscopic polymer melt simulations: non-Rouse behavior of $C_{120}H_{242}$. J Chem Phys 2001; 115(6):2846–59.
[8] Murat M, Kremer K. From many monomers to many polymers: soft ellipsoid model for polymer melts and mixtures. J Chem Phys 1998; 108(10):4340–8.
[9] Louis AA, Bolhuis PG, Hansen JP, Meijer EJ. Can polymer coils be modeled as "soft colloids"? Phys Rev Lett 2000;85(12):2522–5.
[10] Bolhuis PG, Louis AA, Hansen JP. Accurate effective pair potentials for polymer solutions. J Chem Phys 2001;114(9):4296–311.
[11] Reith D, Meyer H, Müller-Plathe F. CG-OPT: a software package for automatic force field design. Comput Phys Commun 2002;148:299–313.
[12] Hoogerbrugge P, Koelman J. Atomistic models of amorphous polybutadienes. Europhys Lett 1992;19(155).
[13] Guerrault X, Rousseau B, Farago J. Dissipative particle dynamics simulations of polymer melts. I. Building potential of mean force for polyethylene and *cis*-polybutadiene. J Chem Phys 2004;121(13):6538–46.
[14] Español P, Serrano M. Dynamical regimes in the dissipative particle dynamics model. Phys Rev E 1999;59(6):6340–7.
[15] Groot RD, Warren PB. Dissipative particle dynamics: bridging the gap between atomistic and mesoscopic simulation. J Chem Phys 1997; 107(11):4423–35.
[16] Soddemann T, Dünweg B, Kremer K. Dissipative particle dynamics: a useful thermostat for equilibrium and nonequilibrium molecular dynamics simulations. Phys Rev E 2003;68:46702–8.
[17] Kindt P, Briels WJ. Scaling of mesoscale simulations of polymer melts with the bare friction coefficient. J Chem Phys 2005;123:224903–9.
[18] Español P, Warren P. Statistical mechanics of dissipative particle dynamics. Europhys Lett 1995;30(4):191–6.
[19] Spenley NA. Scaling laws for polymers in dissipative particle dynamics. Europhys Lett 2000;49(4):534–40.
[20] Shaffer JS. Effects of chain topology on polymer dynamics: Configurational relaxation in polymer melts. J Chem Phys 1995;103(2):761–72.
[21] Paul W, Smith GD, Yoon DY. Static and dynamic properties of a n-$C_{100}H_{202}$ melt from molecular dynamics simulations. Macromolecules 1997;30(25):7772–80.